

Three-dimensional atomic-scale imaging of boron clusters in implanted silicon

O. Cojocaru-Mirédin,^a E. Cadel,^a F. Vurpillot,^a D. Mangelinck^{b,c} and D. Blavette^{a,d,*}

^aUniversité de Rouen, GPM, UMR CNRS 6634 BP 12, Avenue de l'Université, 76801 Saint Etienne de Rouvray, France

^bAix-Marseille Université, IM2NP (UMR 6242) Faculté de Saint-Jérôme – Case 142, F-13397 Marseille, Cedex, France

^cCNRS, IM2NP (UMR 6242) Faculté de Saint-Jérôme – Case 142, F-13397 Marseille, Cedex, France

^dInstitut Universitaire de France, Paris, France

Received 16 July 2008; revised 4 October 2008; accepted 6 October 2008

Available online 21 October 2008

The implantation profile of boron in silicon annealed at 600 °C for 1 h as given by laser-assisted wide-angle atom probe was found to be in good agreement with secondary ion mass spectrometry data. Numerous boron clusters in the form of tiny platelets (3–6 nm diameter, 2 nm thick) were identified and interpreted as boron interstitial clusters (BICs). These BICs contained on average 7 at.% B with a core level that reaches 10 at.%.
© 2008 Acta Materialia Inc. Published by Elsevier Ltd. All rights reserved.

Keywords: Laser atom probe tomography; Microelectronics; Implanted silicon; Boron; Clustering

Boron clustering in boron-implanted silicon is a key issue in microelectronics in the design of the last generation of metal oxide semiconductor field emission transistor (MOS/FET). Ultrashallow junctions a few tens of nanometers deep and extremely highly doped p +/n junctions are needed to continue reducing the size of MOSFET. These doped layers are produced nowadays nearly exclusively by ion implantation which creates defects [1,2]. A thermal treatment is subsequently applied in order to electrically activate dopants (B, P, As). A shallow junction (depth z) obviously leads to an increase in the resistance ($R = 1/\sigma z$ with σ the conductivity) that can be compensated by increasing the conductivity ($\sigma = ce\mu$, where c is the concentration per unit volume, e is the charge of electron and μ is the mobility of the carrier) through a higher dopant concentration (c) that can exceed the solubility limit. After annealing, the implantation peak of boron in silicon is generally found to be immobile and electrically inactive. The origin of this behaviour was interpreted as being due to the presence of boron interstitial clusters (BICs) [3,4] which play an important role in the performance of nanotransistors. However, due to their very small size

(a few nanometers), the chemical composition of these BICs is extremely difficult to determine. The aim of the present study is to clarify the nature of these clusters in supersaturated boron-implanted silicon using a novel approach, the laser-assisted wide-angle tomographic atom probe (LaWaTAP, CAMECA). Implantation profiles as given by LaWaTAP will be compared to secondary ion mass spectrometry (SIMS) profiles.

The use of laser pulses instead of electric pulses in the LaWaTAP makes it possible to analyze materials with low electric conductivity such as silicon or oxides, two key materials for microelectronics [5–8]. The dopant distribution in silicon wafers can routinely be mapped out in three dimensions at the atomic scale [9]. Thompson et al. observed, for instance, the segregation of boron to the grain boundaries in the form of small clusters [10]. The same team observed Cottrell atmospheres of As in implanted silicon at 1000 °C [11].

A high implantation dose was chosen (5×10^{15} atoms cm^{-2} , boron ions of 10 keV) in order to be close to that of ultrashallow junctions. Experiments were conducted on (1 0 0) implanted silicon after annealing at 600 °C for 1 h. Mono-isotopic boron implant (^{11}B) was performed on a boron-doped (1 0 0)-oriented silicon wafer (resistivity 0.01 Ω cm, boron concentration close to 10^{19} atoms cm^{-3}). High aspect ratio, flat-topped 100 μm tall (1 0 0) silicon posts ($5 \times 5 \mu\text{m}^2$) were prepared using Bosch etching techniques [12] on half of

* Corresponding author. Address: Université de Rouen, GPM, UMR CNRS 6634 BP 12, Avenue de l'Université, 76801 Saint Etienne de Rouvray, France. Tel.: +33 2 3285 5035; fax: +33 2 3285 5032; e-mail: didier.blavette@univ-rouen.fr

the wafer in order to prepare sharp tips for LaWaTAP analyses (ion milling using a focused ion beam (FIB)). Implantation was made on these posts and on the other half of the wafer for SIMS investigations. During ion implantation, the silicon substrate was tilted at 7° to the incident ion beam in order to minimize ion channeling effects. A capping layer of silicon was deposited at room temperature on top of samples in order to protect the boron implant from being damaged by the FIB milling during sample preparation. A thermal annealing, for 1 h at 600°C under vacuum at 10^{-6} Torr, was then performed to remove implantation damages and activate dopants. A native oxide 2 nm thick was observed between the protective silicon layer and the implanted silicon substrate.

Tips required for atom probe analysis were made using FIB annular milling [13–15]. Implanted silicon posts were individually transformed into sharply pointed needles ($R \sim 30$ nm) using first a high-energy gallium beam (30 keV). Tips were finally cleaned with a 2 keV gallium beam in order to reduce amorphization and implantation-induced damage. This procedure is described in more details by Thompson et al. [14,15]. The gallium penetration was observed to spread over a distance less than 3 nm with respect to the exposed tip surface. Gallium penetration on the side walls of the needle was, however, observed. In order to avoid gallium irradiation artefacts, depth profiles (Fig. 1) were taken in the inner part of the analysed volume (gallium-free region) where gallium implantation is thought to have almost no influence.

A CAMECA D-SIMS 7f and a CAMECA LaWaTAP were used in conjunction to investigate the distribution of boron atoms in silicon. Boron profiles were measured under vacuum using a primary ion beam of O_2^+ ions with an energy of 3 keV and an impact incidence angle of 45° . The laser implemented in the LaWaTAP was an amplified ytterbium-doped laser ($\lambda = 515$ nm, 350 fs): a pulse of ~ 0.1 μJ was focused onto a spot ~ 0.1 mm in diameter. The projection

parameter used for three-dimensional (3-D) reconstruction of LaWaTAP analyses was the following: $\beta F = 175$ V nm^{-1} ($\beta F = V/R$ with F the evaporation field, β the field factor, V the evaporation voltage and R the tip radius). This parameter was calibrated independently though a calibration of depth scale in experiments where atomic planes were imaged in reconstructed image. The projection factor ($m = 0.6$) that gives the position of the projection centre ($\text{OP} = mR$ with O the centre of the projection sphere and P the projection center) was estimated using field ion microscopy [5]. A more detailed description of reconstruction issues may found elsewhere [16].

The LaWaTAP implantation profile of boron (Fig. 1, log representation) after annealing at 600°C for 1 h reveals that the highest boron level (implantation peak at 9×10^{20} atoms cm^{-3}) is reached at a distance close to 35 nm with respect to the surface. The concentration slowly decreases for larger depths and finally approaches the boron level of the silicon substrate (10^{19} atoms cm^{-3}). The oxygen profile as provided by the LaWaTAP investigation reveals the presence of a 2 nm thick native silicon oxide layer (SiO_2) at the surface of the sample (63 at.% O).

The implantation profile of boron as derived from SIMS experiments, superimposed on the LaWaTAP profile, shows a fairly good agreement between SIMS and LaWaTAP depth profiles. The maximum concentration is detected at a depth of 35 nm in both APT and SIMS profiles. Significant differences are, however, apparent. The LaWaTAP profile indicates a boron concentration of 2×10^{20} atoms cm^{-3} close to the sample surface, whereas the SIMS profile shows a boron concentration of 4.2×10^{20} atoms cm^{-3} , a value that is twice that derived from the LaWaTAP profile. This difference could come from the presence of the native oxide, which can have an influence on SIMS measurements (“matrix effects”) [21]. For depths larger than 75 nm (Fig. 1), the LaWaTAP profile remains slightly above the SIMS profile. This slight discrepancy could come from the implantation procedure of boron which was performed on small area posts for LaWaTAP experiments (silicon posts 5×5 μm^2), whereas SIMS investigations were carried out on large area wafers. The LaWaTAP concentration signal is observed to decrease slowly down to a boron level around $C = 2 \times 10^{19}$ atoms cm^{-3} (400 ppm) at a depth close to 150 nm. This concentration is larger than the detection limits of LaWaTAP for this experiment (close to 8×10^{18} atoms cm^{-3} amu^{-1} or 160 ppm amu^{-1}). The real boron level as given by the difference between the rough concentration and the background noise (over 1 amu) is therefore 1.2×10^{19} atoms cm^{-3} , a value close to the amplitude of the SIMS signal (1×10^{19} atoms cm^{-3}). This latter value is close to the initial boron concentration in the doped Si wafers. The average concentration (i.e. integrated dose) in the implanted region (C), $\sim 2.8 \times 10^{20}$ atoms cm^{-3} , leads to an implantation dose similar to that expected ($Cz \sim 5 \times 10^{15}$ atoms cm^{-2} , where z is the total implantation depth).

Sampling errors in LaWaTAP profiles expressed as atomic fractions (ΔX) are given by the standard deviation $\sigma(\Delta X \sim 2\sigma$ for 5% confidence limit) with

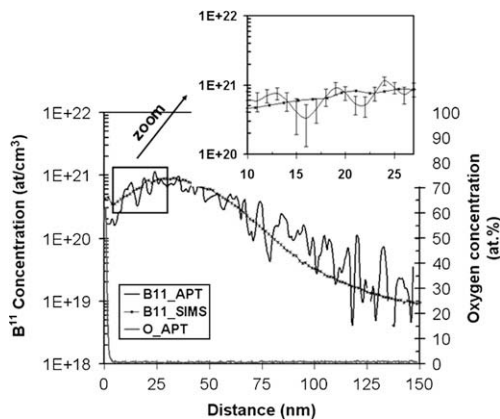


Figure 1. Boron (B^{11}) concentration profile as derived from SIMS and LaWaTAP investigations of boron implanted in silicon after annealing at 600°C for 1 h. The presence of a native oxide at the sample surface is evidenced in the LaWaTAP profile. The depth profiles were drawn by moving a small box (2 nm thick and 12 nm wide) through the analyzed volume (Fig. 2) in a direction perpendicular to the sample surface that was exposed to boron implantation.

$\sigma = (X(1 - X)Q/N)^{1/2}$, where N is the number of detected ions (B + Si) contained in the sampling slice used to construct depth profiles ($N = 7200$ ions/slice). Note that here the detection efficiency ($Q \sim 0.5$) is to be taken into account because it is the statistical fluctuations on local concentration that we wish to estimate (hypergeometric distribution) and not the sampling errors on an estimate of the overall composition of a phase (here the average composition of the implanted region, binomial distribution). For $C = 5 \times 10^{19}$ atoms cm^{-3} , $\Delta C = 2.5 \times 10^{19}$ atoms cm^{-3} .

Although the SIMS and LaWaTAP profiles appear similar, the LaWaTAP profile reveals fine-scale fluctuations of boron concentration that are not visible in the SIMS profile because of the latter's lower spatial resolution (Fig. 1, zoom). These concentration fluctuations are well above the sampling errors and are related to boron clusters that were detected in 3-D LaWaTAP concentration maps. The 3-D concentration field shown in Figure 2 clearly reveals the presence of boron-enriched zones with a high boron concentration (green ~ 6 –7 at.%) compared to the matrix concentration (purple if less than 0.5 at.% or white if zero). Clusters situated in the implantation peak appear as platelets (green envelope). This is more clearly shown in the elemental map of boron atoms (Fig. 2c) where individual boron atoms are represented. As expected, the number density of clusters is significantly higher in the region where the boron concentration is higher (higher driving force for clustering in the implantation peak). The number density of clusters ($\sim 10^{18}$ clusters cm^{-3}) is observed to decrease drasti-

cally for depths exceeding 100 nm. The same trend is observed for sizes: larger clusters, composed of more than 100 atoms, are observed preferentially near the boron peak.

These clusters have the shape of platelets parallel to the implanted surface, in agreement with the high-resolution transmission electron microscopy (HRTEM) observations of BICs by Cristiano et al. who revealed the presence of tiny platelets (5 nm wide) parallel to the implanted surface [3]. These authors identified these platelets as BICs and found that they were small dislocation loops, a few nanometers wide, lying on the (1 0 0) plane parallel to the implanted surface. The Burgers vector of defects indicated that such dislocation loops should contain boron. The anisotropy that is observed in the orientation of BICs (i.e., only platelets parallel to the surface are observed) could be the result of the presence of the surface: these BICs lead to a pronounced deformation of the lattice that can be more easily accommodated when the cluster is parallel to the free surface. Note that this identification of BICs as dislocation loops is in contradiction with the early observations of Wu et al. 30 years ago who reported BICs in the form of rod-like defects [4].

A typical concentration profile drawn perpendicular to a boron-enriched platelet (thickness close to 2 nm) is shown in Figure 3 as an example. This profile was constructed by moving a thin slice perpendicular to a platelet (Fig. 2). This profile shows that the concentration contrast between the cluster and the surrounding matrix is high enough to detect the presence of a cluster and to unambiguously identify its chemical nature. The core composition in the cluster reaches 6 at.% over a distance close to 1 nm, whereas the boron level falls to less than 0.5 at.% in the surrounding silicon matrix. The average boron content in these clusters as determined from LaWaTAP images (depth profiles and/or cluster identification procedure) was found to be close to 7 at.% with a core level that can reach 10 at.% (Fig. 2). These clusters contain a large amount of silicon (~ 90 at.%). Given possible local magnification effects, and the small size of clusters, care should be taken in the interpretation of these measured compositions [17–19]. Images should also in principle be corrected [20]. However, as boron has a high evapora-

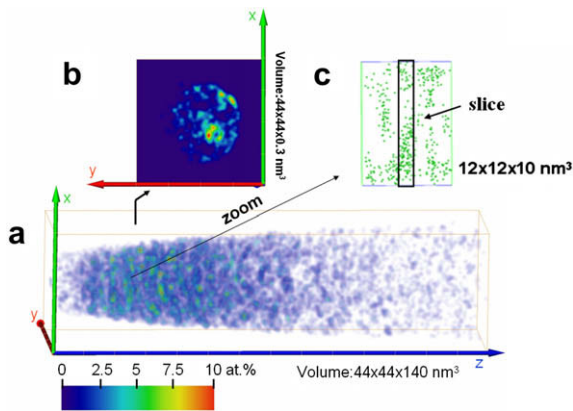


Figure 2. (a) 3-D boron concentration map as derived from LaWaTAP investigations. The reconstructed volume was initially divided in small elemental cubes (1 nm^3) in which the atomic fraction of boron (X) was calculated ($X = N_B/N$, where N_B is the number of boron atoms and N is the total number of atoms contained in the sampling volume). Concentrations were smoothed using a Gaussian window. The atomic fraction of boron (X) is given in false colours (from blue to red (10 at.%) and white when no boron atoms are detected). Tiny boron-enriched clusters with a core concentration close to 10 at.% (red) and a shell (ellipsoidal shape in green) containing around 5 at.% (green) can be seen. (b) Cross-section of the 3-D concentration map given in (a). This image shows the concentration field in a thin slice (0.3 nm) parallel to the sample surface (x, y) at a depth (z) close to the implantation peak (arrow). (c) Enlargement showing the detailed spatial distribution of boron atoms (green dots) in a small region of (a). Clusters clearly appear as platelets (around 6 nm in diameter and 2 nm thick, see depth profile shown in Fig. 3).

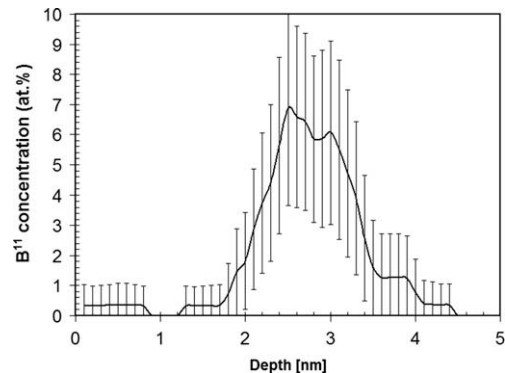


Figure 3. The boron concentration profile through a cluster (the sampling box is a small slice ($3 \times 3 \times 0.1 \text{ nm}^3$)). Bars give the sampling errors (2σ).

tion field compared to silicon, ion trajectories are divergent. As a result, the core of boron-enriched zone in 3-D images is much less prone to ion trajectory overlaps: the core should be free from ions coming from the surrounding silicon matrix. The composition of the inner part of imaged clusters (7–10 at.%) is thought to be representative of the real boron concentration in clusters. These boron clusters are likely to be non-equilibrium nuclei formed after annealing at 600 °C and identified in the microelectronics community as BICs. Compared to the HRTEM observations of Cristiano et al., platelets observed with LaWaTAP are thicker. Even so, HRTEM images show a single layer of interstitial atoms, the presence of boron around the dislocation loop cannot be ruled out. Reconstruction artefacts in LaWaTAP could also slightly enlarge the thickness of boron-enriched zones.

As a conclusion, the redistribution of boron in implanted monocrystalline silicon (10 keV; 5×10^{15} atoms cm^{-2}) annealed at 600 °C for 1 h has been studied using both LaWaTAP and SIMS. The boron concentration was found to increase steeply to 10^{21} atoms cm^{-3} at a distance close to 35 nm and to decrease slowly to 10^{19} atoms cm^{-3} , a value close to the boron level of the silicon substrate. The implantation profile of boron as given by LaWaTAP analysis was found to be in reasonable agreement with SIMS data. Numerous boron clusters identified as BICs (platelets 3–6 nm in diameter, 2 nm thick) and containing between 50 and 300 atoms (Si and B) were clearly observed in 3-D reconstructed volumes. This number of atoms is found to be much higher than that generally assumed, in particular in *ab initio* modelling. These clusters form as a result of the large boron concentration (above 10^{19} atoms cm^{-3}) compared to the limit solubility of B in Si at 600 °C (5×10^{17} atoms cm^{-3}) [21]. These clusters contain on average ~ 7 at.% B with a core that can contain up to 10 at.% B.

The authors wish to thank B. Duployer and A. Portavoce (IM2NP, Marseille) for their help in this work. Many thanks also to R. Daineche who carried out SIMS analyses.

- [1] G.Z. Pan, R.P. Ostroumov, L.P. Ren, Y.G. Lian, K.L. Wang, *J. Non-Crystalline Solids* 352 (2006) 2506.
- [2] P. Calvo, A. Claverie, N. Cherkashin, B. Colombeau, Y. Lamrani, B. de Mauduit, F. Cristiano, *Nuclear Instr. Meth. Phys. Res. B* 216 (2004) 173.
- [3] F. Cristiano, X. Hebras, N. Cherkashin, A. Claverie, *Appl. Phys. Lett.* 83 (2003) 5407.
- [4] W.K. Wu, J. Washburn, *Crys. Lattice Defects* 7 (1977) 39.
- [5] A. Cerezo, T.J. Godfrey, S.J. Sijbrandij, G.D.W. Smith, P.J. Warren, *Rev. Sci. Instrum.* 69 (1998) 49.
- [6] T.F. Kelly, M.K. Miller, *Rev. Sci. Instrum.* 78 (2007) 031101.
- [7] B. Deconihout, F. Vurpillot, B. Gault, G. Da costa, M. Bouet, A. Bostel, D. Blavette, A. Hideur, G. Martel, M. Brunel, *Surf. Interf. Anal.* 39 (2007) 278–282.
- [8] B. Gault, F. Vurpillot, M. Gilbert, A. Vella, A. Menand, D. Blavette, B. Deconihout, *Rev. Sci. Instrum.* 77 (2006) 043705.
- [9] K. Thompson, J.H. Bunton, T.F. Kelly, D.J. Larson, *J. Vac. Sci. Technol. B* 24 (1) (2006) 421–427.
- [10] K. Thompson, J. Booske, D.J. Larson, T.F. Kelly, *Appl. Phys. Lett.* 87 (2005) 052108.
- [11] K. Thompson, P.L. Flaitz, P. Ronsheim, D.J. Larson, T.F. Kelly, *Science* 317 (2007) 1370.
- [12] A.A. Ayron, R. Braff, C.C. Lin, H.H. Swain, M.A. Schmidt, *J. Electrochem. Soc.* 146 (1) (1999) 339.
- [13] D.J. Larson, D.T. Foord, A.K. Petford-Long, H. Liew, M.G. Blamire, A. Cerezo, G.D.W. Smith, *Ultramicroscopy* 79 (1999) 287.
- [14] Thompson et al., *Ultramicroscopy* 107 (2–3) (2006) 131.
- [15] Thompson et al., *Microsc. Microanal.* 12 (S2) (2006) 1736CD.
- [16] P. Bas, A. Bostel, B. Deconihout, D. Blavette, *Appl. Surf. Sci.* 87/88 (1995) 298–304.
- [17] F. Vurpillot, A. Bostel, D. Blavette, *Appl. Phys. Lett.* 76–21 (2000) 3127–3129.
- [18] D. Blavette, E. Cadel, A. Fraczkiewicz, A. Menand, *Science* 17 (1999) 2317–2319.
- [19] D. Blavette, F. Vurpillot, P. Pareige, A. Menand, *Ultramicroscopy* 89 (2001) 145–153.
- [20] F. De Geuser, W. Lefebvre, F. Danoix, F. Vurpillot, B. Forbord, D. Blavette, *Surf. Interf. Anal.* 39 (2007) 268–272.
- [21] D. Nobili, *Properties of Silicon, EMIS data reviews series No. 4, INSPEC publication, 1988, pp. 384–385.*